N89-15947

# TRAJECTORY COMPUTATION DURING A MANEUVER: THRUST ESTIMATION WITH THE GODDARD TRAJECTORY DETERMINATION SYSTEM (GTDS)*

A. C. Beri and M. V. Samii, Computer Sciences Corporation (CSC)
C. E. Doll, Goddard Space Flight Center (GSFC)

ABSTRACT

Existing thrust modeling capabilities of the Goddard Trajectory Determination System (GTDS) have been enhanced to allow calibration of the onboard propulsion system. These enhancements provide one or more thrust scale factors, based on estimation using the batch least-squares technique, for the case of along-track thrust and the case of attitude-dependent thrust. The enhancements are evaluated using simulated tracking measurements for a test spacecraft and using actual tracking measurements for the Earth Radiation Budget Satellite (ERBS). The effects of tracking measurement noise and distribution on the accuracy of the estimation are investigated and found to be significant. Results and conclusions of the analysis are presented.

*This work was supported by the National Aeronautics and Space Administration (NASA)/Goddard Space Flight Center (GSFC), Greenbelt, Maryland, under Contract NAS 5-31500.

# 1. INTRODUCTION

The force modeling requirements for trajectory computation for spacecraft supported by the Flight Dynamics Facility (FDF) at the Goddard Space Flight Center (GSFC) are different for each mission phase (Reference 1). The forces that determine the trajectory of the spacecraft during the on-orbit phase include solar, lunar, and Earth gravitational forces; aerodynamic forces; and solar radiation effects. These forces are continuously in effect and are modeled generically for all spacecraft. Trajectory computation during maneuvers, such as transfer orbit, stationkeeping, and targeting, involves modeling the force due to thrust, which is different for different spacecraft and types of maneuvers. Two thrust models, one dealing with along-track thrust and the other with attitude-dependent thrust, have recently been implemented and tested as enhancements to the Goddard Trajectory Determination System (GTDS). These models are the subject of this paper.

The paper is organized into four sections. The remainder of Section 1 discusses the scope and goals of the paper and describes the current thrust estimation capabilities in GTDS and the current and future thrust estimation requirements. Sections 2 and 3 discuss the along-track thrust estimation model and the attitude-dependent thrust estimation model, respectively; each of these sections includes a description of the estimation method, a discussion of the estimation results, and the conclusions. Section 4 describes future developments in thrust estimation.

## 1.1 SCOPE AND GOALS

This paper discusses force modeling in GTDS for the case of along-track thrust and for the case of thrust with cross-track or radial components. The mathematical formulation of the thrust estimation algorithm and evaluation of the resulting enhanced GTDS are presented. The goals of the evaluation are the following:

- To establish whether a reliable postburn state can be determined

- To assess the influence of tracking measurement noise, tracking measurement distribution, and the a priori state vector on thrust estimation

## 1.2 CURRENT THRUST ESTIMATION CAPABILITIES IN GTDS

The inclusion of thrust forces in GTDS allows powered ephemeris generation through the Ephemeris Generation (EPHEM) Program and thrust level estimation through the Differential Correction (DC) Program. Thrust estimation is currently supported by GTDS in the form of a polynomial thrust option, which allows variation of eight or less polynomial coefficients $a_i$ of the thrust acceleration function, A(t), written as

$$A(t) = \sum_{i=1}^{8} a_i \, t^{i-1} \tag{1}$$

where t is the time from ignition (Reference 2). The thrust estimation can be performed in conjunction with attitude estimation (or specification). Variations in the spacecraft roll, pitch, and yaw, or in the right ascension and declination, as functions of time are each represented as polynomials of order four or less, with variable coefficients. These coefficients can also be estimated in the DC Program.

In the DC Program, the spacecraft a priori state can always be estimated. However, if the a priori state is known to be highly accurate, its variation can be suppressed, thus allowing the differential correction process to vary only the thrust scale factor. In general, this can be expected to provide a more reliable estimated thrust factor.

## 1.3 CURRENT AND FUTURE THRUST MODELING REQUIREMENTS

For several National Aeronautics and Space Administration (NASA) missions, such as the Cosmic Background Explorer (COBE) and Geostationary Operational Environmental Satellite (GOES), it is desirable to perform near-realtime calibration of the onboard propulsion system. Thus, If $A_{nom}(t)$ is the nominal thrust acceleration measured under controlled conditions and $A_{eff}(t)$ is the actual effective thrust acceleration during maneuvers, then a calibration factor $(1 + \tau)$ is required, such that

$$A_{eff}(t) = (1 + \tau)\, A_{nom}(t) \tag{2}$$

The polynomial thrust estimation option currently operational in GTDS potentially changes the form of the nominal thrust profile by allowing independent variation of all the coefficients. It does not allow estimation of the single calibration factor of Equation (2). A desirable enhancement would include an arbitrary profile for $A_{nom}(t)$ (e.g., thrust input in the form of a numerical table of thrust acceleration values) and the capability to estimate a calibration factor $(1 + \tau)$. Since the maneuvers are often accompanied by highly specific attitude configurations, a generalization of the attitude specification and estimation is also important. These issues are discussed further in Sections 2 and 3.

## 2. ESTIMATION OF ALONG-TRACK THRUST

This section presents a discussion of thrust estimation for the case of thrust entirely along the velocity direction (along-track). In GTDS, this involves the inclusion of an additional term in the force model to account for the thrust, as well as the specification of a thrust scale factor $(1 + \tau)$ to be estimated.

Several factors influence the thrust estimation process, such as the nature of the tracking measurements used for estimation (i.e., length of data arc, distribution, biases, noise), the reliability of the a priori state vector, and the number of parameters being simultaneously estimated. Functional feasibility of the enhanced GTDS can be established by evaluating the influence of these factors on the system.

The thrust estimation method is described in Section 2.1. The results of the evaluation and the conclusions of the analysis are presented in Sections 2.2 and 2.3, respectively. Further information can be found in References 3 and 4.

## 2.1 METHOD FOR ALONG-TRACK THRUST ESTIMATION

The enhanced GTDS thrust force model described in this section [referred to as the tabular thrust force model (TTFM)] uses the existing thrust magnitude coefficient estimation function in GTDS to enhance the capability of the polynomial thrust model. In this force model, the jth acceleration vector at time $t_i$, $\vec{A}_j(t_i)$, which is assumed to be aligned with the velocity of the spacecraft in the orbit plane coordinate system, can be written as follows:

$$\vec{A}_j(t_i) = (1 + \tau_j)\left[\frac{F_j(t_i)}{M_j(t_i)}\right]\hat{v} \tag{3}$$

where $\hat{v}$ = velocity unit vector

$F_j(t_i)$ = jth thrust force magnitude at time $t_i$

$M_j(t_i)$ = corresponding mass of the spacecraft during the jth thrust at time $t_i$

$\tau_j$ = thrust variation coefficient of the jth thrust

A maximum of 20 thrust forces can be modeled, each thrust being represented by a thrust table and a corresponding mass table.

One of two options, an application option or an estimation option, can be specified. If the application option is chosen for a particular thrust, for example the jth thrust, then $\tau_j$ is automatically set to zero, and the thrust and mass tables of the jth thrust are used in calculating the acceleration, $\vec{A}_j$, to be applied. If, however, the estimation option is chosen, then the best estimates of $\tau_j$ are determined by GTDS as solve-for parameters.

The TTFM is capable of applying and estimating thrust levels simultaneously. However, within this model thrust can be applied or estimated only in the spacecraft velocity direction. This limitation could be removed in several ways, one of which is discussed in Section 3 of this paper. Thrust estimation in GTDS involves the incorporation of the thrust levels in the total force function and the inclusion of the coefficients $\tau_i$ in the variational process. References 1, 3, and 4 provided detailed descriptions of the mathematical and computational procedures employed by GTDS for this estimation.

## 2.2 RESULTS AND DISCUSSION

In evaluating the TTFM, tests were performed to determine how well the thrust was estimated under different conditions. Specifically, the effects of the following operational conditions were studied:

- Input Thrust Level--The input thrust level can range from 0 percent to 100 percent of the "actual" thrust.

- State Estimation--Estimation of the state may or may not be performed in conjunction with thrust estimation.

- Tracking Measurement Quality--The quality of the tracking measurement can be high or low due to noise and biases.

- Tracking Measurement Distribution--The distribution of tracking measurements may be good, with a large number of passes uniformly distributed throughout the orbit determination data arc, or the distribution may be poor, with a few passes clustered together and large gaps with no tracking measurements.

- Data Arc Length--The data arc length can be small or large compared with a period during which the tracking geometry changes significantly.

Within this evaluation framework, TTFM was tested in two stages. In the first stage, the overall accuracy and reliability of TTFM was tested through thrust analysis under controlled conditions for a typical mission, called TEST, whose ascent phase includes a series of short burns, followed by longer burns. These burns were modeled by the Generalized Maneuver (GMAN) Program, which generates tables of thrust as a function of time for specified engine parameters. The tracking schedule and associated Tracking and Data Relay Satellite System (TDRSS) tracking measurements were simulated, with <u>known</u> thrust profiles included in the force model used by the simulation.

The single ideal thrust coefficient, $\tau$, can be predicted exactly for this case, independently of the TTFM, and the difference between the actual estimated $\tau$ determined by the TTFM and the ideal $\tau$ provides a measure of the accuracy and reliability of the TTFM.

The second stage of TTFM testing involved performing tests to support orbit analysis for the ERBS ascent-phase maneuvers using actual Ground Spaceflight and Tracking Data Network (GSTDN) tracking measurements taken on October 7 and 8, 1984. The TTFM was applied to the 183-minute calibration burn and to the first long 376-minute burn to evaluate the performance of the TTFM using actual tracking measurements. Since the actual thrust is not known exactly for this case, these tests do not measure the accuracy of thrust estimation with the TTFM. The results for TEST and ERBS are discussed in Sections 2.2.1 and 2.2.2, respectively.

### 2.2.1 TEST ANALYSIS RESULTS

To evaluate the accuracy and relibility of the TTFM, GTDS was modified to include the enhanced thrust capabilities based on the TTFM. The TTFM was tested on two types of maneuvers: (1) brief (70-second) maneuvers that raise the TEST orbit by about 1 kilometer and (2) long-burn (94-minute) maneuvers that raise the TEST orbit by about 200 kilometers.

Tests of the accuracy of the thrust estimation were performed as follows:

- Simulated tracking measurements were generated with a force model containing known nominal thrust accelerations $A_j(t)$, one of which, $A_{nom}(t)$, is to be estimated [Equation (3)].

- GTDS was executed using the TTFM, with the particular input thrust level, $A_{in}(t)$, different from $A_{nom}(t)$ by a factor $\phi$, i.e.,

$$A_{in}(t) = \phi \, A_{nom}(t) \tag{4}$$

- The thrust scale factor $(1 + \tau)$ estimated by GTDS was then examined; this scale factor defines the final estimated thrust, $A_{est}(t)$, in terms of $A_{in}(t)$, as follows:

$$A_{est}(t) = (1 + \tau) \, A_{in}(t) \tag{5}$$

Under ideal estimation conditions, since the tracking measurements reflect a thrust $A_{nom}(t)$, then $A_{est}(t)$ must equal $A_{nom}(t)$, i.e.,

$$A_{est}(t) = A_{nom}(t) \tag{6}$$

Or, using Equations (5) and (4),

$$(1 + \tau) \, A_{in}(t) = A_{nom}(t) \tag{7}$$

$$(1 + \tau) \, \phi \, A_{nom}(t) = A_{nom}(t) \tag{8}$$

Thus, for ideal thrust estimation, the following condition must be satisfied:

$$(1 + \tau) \, \phi = 1 \tag{9}$$

Therefore, the evaluation criterion for ideal thrust estimation is

$$\tau = \frac{1}{\phi} - 1 \tag{10}$$

2.2.1.1 Short-Maneuver Results

The Research and Development (R&D) GTDS Program was used to generate simulated Tracking and Data Relay Satellite-East (TDRS-E) and TDRS-West (TDRS-W) tracking measurements for TEST for a total data arc span of 3 hours and 20 minutes, starting at 1 hour and 30 minutes (Figure 1). There were a total of 13 passes, eight tracked by TDRS-E and five tracked by TDRS-W. Range and Doppler data generated at 10-second intervals formed passes 8 minutes long.

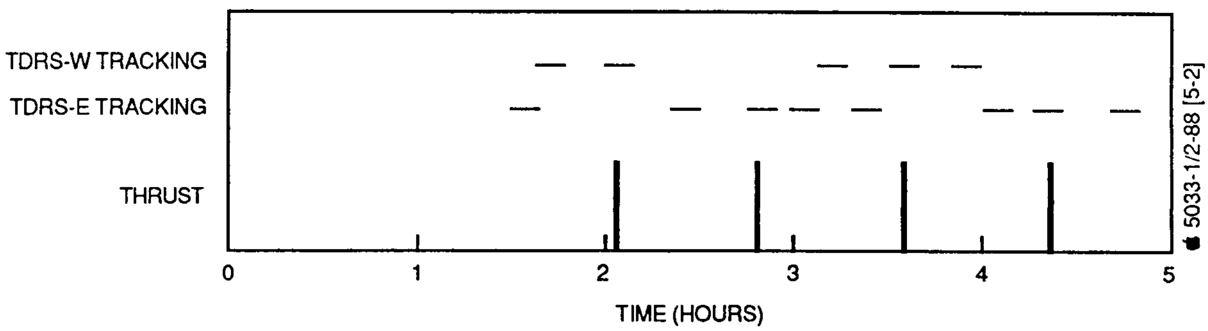


Figure 1. Simulated TDRS-W and TDRS-E Tracking Measurement Passes for TEST Short Maneuvers and the Associated Thrust Pattern

The TTFM was tested for several cases using the 70-second TEST maneuvers. Each of the four thrusts was estimated in separate executions, with 90 percent of the thrust magnitude used as input to GTDS, corresponding to $\phi = 0.9$. For each test, the remaining three thrusts were applied with $\tau_j = 0$ [Equation (3)]. From Equation (10), the value of $\tau$ expected for the case of ideal thrust estimation is 0.111111.

The results of simultaneously solving for the state and thrust for each short maneuver are given in Table 1. The estimated values of $\tau$ agree with the expected value of 0.111111 to better than 1 percent, establishing the functional reliability of the TTFM. The estimated values of the state components agree with their a priori values at epoch to within 1 meter in position and to within $10^{-3}$ meter per second in velocity for three of the four maneuvers. The larger differences seen for the first thrust are due to the greater cumulative effect of an early force perturbation on the overall trajectory, relative to later ones. However, the maximum 4-meter difference in position is still within quality assurance standards.

2.2.1.2 Long-Burn Results

The TEST ascent phase includes a number of long-burn, low-thrust maneuvers. Since each one of these burns typically takes more than an hour, the thrust level and state estimation during the burn can allow adjustments to the thrust that may be necessary for proper orbit raising or stationkeeping.

TEST thrust level estimation during the ascent phase was utilized to evaluate the TTFM using simulated TDRSS two-way Doppler data. The tracking schedule assumed for the first long burn of 94 minutes is depicted in Figure 2. It

Table 1. State and Thrust Estimation for TEST During Short Maneuvers

| THRUST NO. | DIFFERENCE BETWEEN FINAL AND A PRIORI STATE | | | | | | THRUST SCALE FACTOR, $\tau$ |
|---|---|---|---|---|---|---|---|
| | $\Delta X$ (METERS) | $\Delta Y$ (METERS) | $\Delta Z$ (METERS) | $\Delta \dot{X}$ (METERS/SECOND) | $\Delta \dot{Y}$ (METERS/SECOND) | $\Delta \dot{Z}$ (METERS/SECOND) | |
| 1 | −3.6 | −0.35 | 3.2 | −0.00307 | 0.00093 | −0.0049 | 0.1118 |
| 2 | −0.04 | 0.14 | −0.26 | −0.00007 | 0.00005 | 0.00043 | 0.1112 |
| 3 | 0.27 | 0.15 | −0.42 | 0.00015 | −0.00002 | 0.00062 | 0.1112 |
| 4 | 0.37 | 0.17 | −0.49 | 0.00026 | −0.00003 | 0.00076 | 0.1117 |

5033-16/2-88[5-2]

NOTES: 1. 13 PASSES (8 TDRS-E, 5 TDRS-W) DURING $3^h 20^m$ DATA ARC
2. RANGE AND DOPPLER OBSERVATIONS OF TEST
3. SOLVE FOR STATE AND -10% PERTURBED SINGLE THRUST

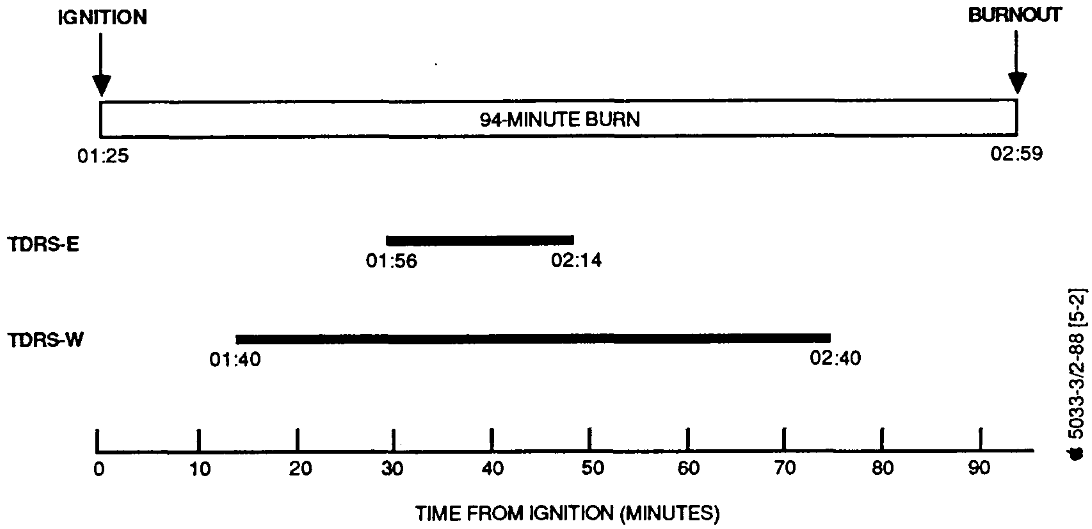


Figure 2. Simulated TDRS-E and TDRS-W Tracking Measurement Passes for the TEST Long-Burn Maneuver and the Associated Thrust

consists of one 18-minute TDRS-E pass starting from 31 minutes after ignition and one 60-minute TDRS-W pass starting from 15 minutes after ignition.

Two sets of simulated tracking measurements were generated, one with and one without measurement noise (a measurement noise standard deviation of 0.25 hertz was assumed). Initial state errors introduced in the GTDS DC Program input were assumed to be in the along-track direction (100 meters and 10 centimeters per second for the TEST spacecraft and 50 meters and 1 centimeter per second for TDRS-E and TDRS-W).

Thrust estimation was performed for the 14 tracking measurement distributions given in Figure 3. For the distributions E1(9), E1(18), W1(10), W6(10), and W16(20) shown in Figure 3, the following combinations of measurement noise and initial state error were included:

- o: No measurement noise
- a: Measurement noise

- b: Measurement noise and TEST initial state error
- c: Measurement noise, TEST initial state error, and TDRS initial state error

The results for $\tau$ and the position error at burnout and at 3 hours from burnout are presented in Tables 2 and 3. Table 2 compares the o, a, b, c results for the specific tracking scenarios and illustrates the effects of noise and TEST or TDRS initial state errors on the estimation. The results presented in Table 3 include noise and the TEST initial state error and illustrate the effects of the location of tracking measurements and the length of the measurement pass.

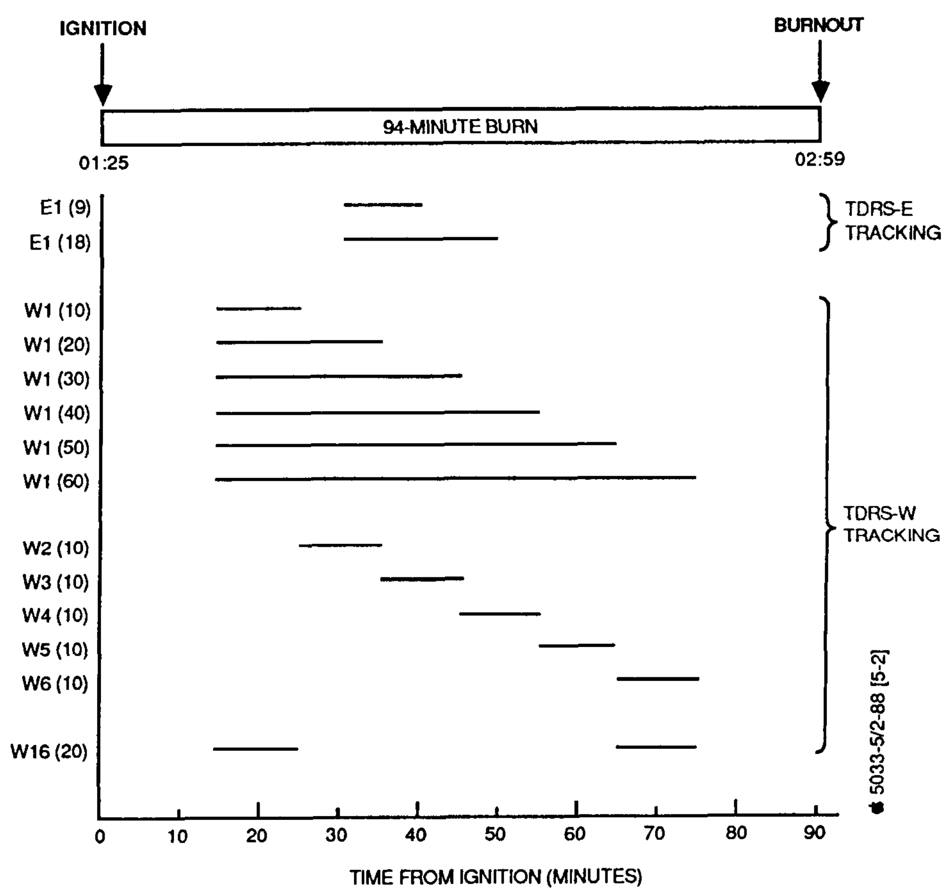


Figure 3. Tracking Measurement Distributions Used for Evaluation of TEST Long-Burn Thrust Estimation

Table 2. Effects of Noise and TEST and TDRS Initial State Errors on Thrust Estimation During the TEST Long Burn

| TRACKING MEASUREMENT DISTRIBUTION* | FINAL THRUST SCALE FACTOR, $\tau$ | POSITION ERRORS (METERS) | |
|---|---|---|---|
| | | AT BURNOUT | AT 3 HOURS FROM BURNOUT |
| E1(9)[o] | 0.11101 | 52 | 299 |
| E1(9)[a] | 0.11143 | 149 | 1,440 |
| E1(9)[b] | 0.11596 | 1,499 | 17,718 |
| E1(9)[c] | 0.11624 | 4,243 | 19,508 |
| E1(18)[o] | 0.11105 | 27 | 160 |
| E1(18)[a] | 0.11122 | 42 | 443 |
| E1(18)[b] | 0.11368 | 781 | 9,292 |
| E1(18)[c] | 0.11450 | 2,900 | 13,099 |
| W1(10)[o] | 0.11088 | 198 | 816 |
| W1(10)[a] | 0.11219 | 440 | 4,536 |
| W1(10)[b] | 0.12743 | 5,905 | 64,296 |
| W1(10)[c] | 0.10451 | 7,064 | 30,604 |
| W6(10)[o] | 0.11105 | 19 | 152 |
| W6(10)[a] | 0.11107 | 11 | 156 |
| W6(10)[b] | 0.11355 | 563 | 7,842 |
| W6(10)[c] | 0.11591 | 3,548 | 16,968 |
| W16(20)[o] | 0.11106 | 12 | 116 |
| W16(20)[a] | 0.11109 | 11 | 69 |
| W16(20)[b] | 0.11266 | 1,017 | 4,925 |
| W16(20)[c] | 0.11686 | 4,156 | 20,090 |

5033-15/2-88[5-2]

*SEE FIGURE 3. THE NUMBERS IN PARENTHESES REPRESENT THE TOTAL DURATION MEASUREMENTS IN MINUTES. SUPERCRIPTS o,a,b,c INDICATE THE FOLLOWING:

o = NO MEASUREMENT NOISE
a = MEASUREMENT NOISE
b = MEASUREMENT NOISE AND TEST INITIAL STATE ERROR
c = MEASUREMENT NOISE, TEST INITIAL STATE ERROR, AND TDRS INITIAL STATE ERROR

Table 3. Effects of Data Arc Location and Length on Thrust Estimation During the TEST Long Burn

| SOLUTION ARC* | ARC LENGTH (MINUTES) | FINAL THRUST SCALE FACTOR, $\tau$ | POSITION ERRORS (METERS) AT BURNOUT | POSITION ERRORS (METERS) AT 3 HOURS FROM BURNOUT |
|---|---|---|---|---|
| W1(10)[b] | 10 | 0.12743 | 5,905 | 64,296 |
| W1(20)[b] | 20 | 0.12328 | 10,282 | 47,336 |
| W1(30)[b] | 30 | 0.11496 | 3,005 | 14,041 |
| W1(40)[b] | 40 | 0.11272 | 1,266 | 5,744 |
| W1(50)[b] | 50 | 0.11184 | 668 | 2,748 |
| W1(60)[b] | 60 | 0.11146 | 444 | 1,538 |
| W1(10)[b] | 10 | 0.12743 | 5,905 | 64,296 |
| W2(10)[b] | 10 | 0.12393 | 10,786 | 49,736 |
| W3(10)[b] | 10 | 0.11600 | 3,732 | 17,649 |
| W4(10)[b] | 10 | 0.11398 | 2,099 | 9,965 |
| W5(10)[b] | 10 | 0.11355 | 563 | 7,842 |
| W6(10)[b] | 10 | 0.11326 | 1,045 | 5,801 |

5033-6/2-88[5-2]

*SEE FIGURE 3. THE NUMBERS IN PARENTHESES REPRESENT THE TOTAL DURATION OF MEASUREMENTS IN MINUTES. SUPERCRIPTS o, a, b, c INDICATE THE FOLLOWING:

o = NO MEASUREMENT NOISE
a = MEASUREMENT NOISE
b = MEASUREMENT NOISE AND TEST INITIAL STATE ERROR
c = MEASUREMENT NOISE, TEST INITIAL STATE ERROR, AND TDRS INITIAL STATE ERROR

As can be seen from Table 2, measurement noise does not appear to be significant in the estimation process, but the presence of TEST and/or TDRS initial state errors introduces noticeable deterioration of the quality of the orbit determination results. The overall orbital accuracy, however, is expected to satisfy the operational orbit support requirements. Table 3 shows that the observability of $\tau$ improves and, thus, the overall orbit determination accuracy improves as the length of the data arc increases or, in the case of a constant-length data arc, as the data are placed farther away from ignition.

### 2.2.2 ERBS ASCENT-PHASE ANALYSIS RESULTS

The TTFM was tested using real GSTDN tracking data for ERBS. The first part of the study focused on the calibration burn and on the 8.5-hour free-flight interval immediately following that burn. The second part of the study focused on the first long burn and on the subsequent 5-hour free flight. The tracking distribution for the duration of the study is shown in Figure 4. Passes C1 through C16 are used in the calibration study, and passes L1 through L10 are used in the long-burn study.

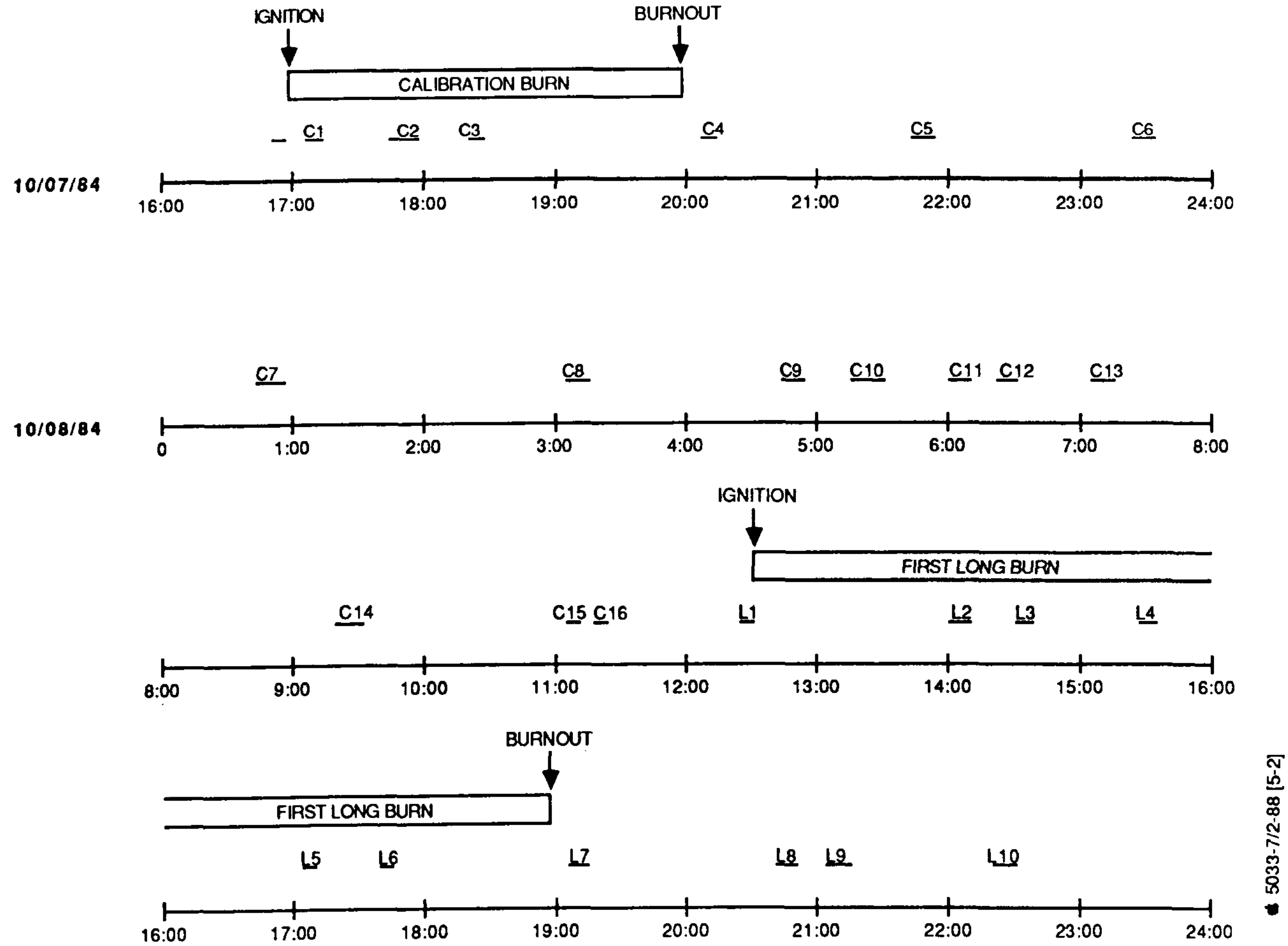


Figure 4. Tracking Measurement Distribution During the Calibration Burn and the First Long Burn of the ERBS Ascent Phase

During the ERBS analysis, thrust estimation was evaluated by comparing ephemerides [using the GTDS Ephemeris Comparison (COMPARE) Program] propagated from state vectors estimated under various conditions. These conditions included the following:

- Different distributions of tracking measurement passes.

- Different levels of constraint on the variation of the a priori state, through the state covariance matrix. (The a priori state is effectively fixed when a covariance constraint is applied, i.e., when very small values are used for the elements of the state covariance matrix.)

- Solutions based on tracking measurement taken during powered flight and those based on free-flight data.

The following evaluation criteria were used in comparing the results for the various cases:

- Consistency in the estimated value of $\tau$

- Final value of the weighted root mean square (WRMS) of the observed-minus-computed (O-C) residuals, i.e., the differences between the actual tracking observations O and the computed (estimated) observations C

- Consistency in the differences between the ephemerides propagated from each solution and a reference ephemeris at different times on the solution arc

2.2.2.1 Calibration Burn Results

Using an epoch vector at the ignition of the calibration burn on October 7, 1984, at 16 hours, 53 minutes, a reference ephemeris (solution n) was generated using the nominal thrust level modeled by the GMAN Program. Utilizing the same epoch vector, thrust estimation was performed and the ephemeris propagated to the start of the first long burn. This was done for four cases, as follows:

1. Solution using pass C1 (with initial state covariance constraints)

2. Solution using passes C1 and C2 (with initial state covariance constraints)

3. Solution using passes C1, C2, and C3 (with initial state covariance constraints)

4. Solution using passes C1, C2, and C3 (with no initial state covariance constraints)

A fifth solution (solution 5) was a postburn, free-flight solution using passes C4 through C16 (with no initial state covariance constraints) and an epoch at 19 hours, 58 minutes.

The results for $\tau$ are summarized in Table 4. The most notable result is the convergence of $\tau$ as the number of observations increases. The value of $\tau$ from solution 3 was chosen to calculate a thrust calibration factor for the first long-burn flight segment. Solution 3 was obtained using a fixed a priori state and the greatest number of observations, thus making the corresponding thrust scale factor the most accurate. This conclusion is based on the analysis described in References 3 and 4. The larger WRMS for solutions 1, 2, and 3, compared with that for solution 4, results from poor trajectory estimation (because of the constrained initial state) for solutions 1, 2, and 3.

The GTDS COMPARE Program was used to compare solutions 1 through 4 with the reference solution and with the free-flight solution. The results are presented in Table 5. It is clear from this table that solution 1 is not acceptable. The large position error associated with this solution is due

Table 4. Results of Thrust Variation Coefficient Estimations for the ERBS Calibration Burn

| SOLUTION | NO. OF PASSES | NO. OF OBSERVATIONS | FINAL THRUST SCALE FACTOR, $\tau$ | NO. OF ITERATIONS | WRMS | COVARIANCE CONSTRAINTS |
|---|---|---|---|---|---|---|
| 1 | 1 | 31 | − 0.328 | 3 | 14.166 | YES |
| 2 | 2 | 67 | − 0.127 | 4 | 16.355 | YES |
| 3 | 3 | 156 | − 0.117 | 4 | 12.097 | YES |
| 4 | 3 | 139 | − 0.113 | 5 | 1.338 | NO |

5033-8/2-88[5-2]

Table 5. Comparisons of Along-Track Position Differences for the ERBS Calibration Burn

**a. COMPARISON WITH THE REFERENCE EPHEMERIS SOLUTION (SOLUTION n)**

| SOLUTION COMPARED | ALONG-TRACK POSITION DIFFERENCES (KILOMETERS) | | | | | |
|---|---|---|---|---|---|---|
| | DURING BURN | | DURING FREE-FLIGHT | | | |
| | $16^h\ 58^m$ | $18^h\ 28^m$ | $19^h\ 58^m$ | $21^h\ 18^m$ | $22^h\ 38^m$ | $23^h\ 58^m$ |
| 1 | - 0.098209 | 52.23137 | 197.1167 | 357.8751 | 519.0224 | 680.5509 |
| 2 | - 0.252476 | 13.35632 | 57.5685 | 107.1451 | 157.1803 | 207.7262 |
| 3 | - 0.190235 | 12.83301 | 53.5299 | 98.9438 | 144.5701 | 190.5996 |
| 4 | - 0.385551 | 12.82878 | 52.4604 | 96.6848 | 141.1091 | 185.9451 |

**b. COMPARISON WITH THE FREE-FLIGHT SOLUTION (SOLUTION 5)**

| SOLUTION COMPARED | ALONG-TRACK POSITION DIFFERENCES (KILOMETERS) | | | |
|---|---|---|---|---|
| | $19^h\ 58^m$ | $21^h\ 18^m$ | $22^h\ 38^m$ | $23^h\ 58^m$ |
| 1 | 139.1953 | 254.0555 | 369.3852 | 485.3086 |
| 2 | 0.0929 | 4.0365 | 8.3164 | 13.0124 |
| 3 | - 3.9413 | - 4.1571 | - 4.2851 | - 4.1084 |
| 4 | - 4.9910 | - 6.3822 | - 7.7053 | - 8.7258 |

5033-9/2-88 [5-2]

to the poor estimate of $\tau$ as discussed earlier. The other comparison results shown in Table 4 are all consistent and represent reliable estimation.

### 2.2.2.2 First Long-Burn Results

Thrust estimation was performed for the ERBS first long burn using the TTFM and an evaluation plan similar to that for the calibration burn. An epoch vector at the ignition of the first long burn was obtained from calibration solution 5. A reference ephemeris was generated along with a series of DC Program and EPHEM Program solutions, extending to 5 hours after the end of the burn. A value of $\tau$ equal to -0.117 (from calibration burn solution 3, see Table 4) was used to scale the input thrust used in this part of the study. The new value of $\tau$, estimated with the calibrated thrust as input, should be close to zero.

The results of the first-long-burn study are summarized in Table 6. Solutions A through F in this table are based on the following tracking measurement distributions:

A. Solution using passes L2 and L3 (with initial state covariance constraint)

B. Solution using passes L3 and L4 (with initial state covariance constraint)

C. Solution using passes L2 through L6 (with initial state covariance constraint)

D. Solution using passes L2, L5, L6, L9 (with no initial state covariance constraint)

E. Solution using passes L2 through L10 (with no initial state covariance constraint)

F. Postburn, free-flight solution using passes L7 through L10 (with no initial state covariance constraint)

Table 6. Results of Thrust Variation Coefficient Estimations for the ERBS First Long Burn

| SOLUTION | NO. OF PASSES | NO. OF OBSERVATIONS | FINAL THRUST SCALE FACTOR, $\tau$ | NO. OF ITERATIONS | WRMS | COVARIANCE CONSTRAINTS |
|---|---|---|---|---|---|---|
| A | 2 | 126 | −0.0188 | 4 | 3.030 | YES |
| B | 2 | 67 | −0.0208 | 4 | 4.519 | YES |
| C | 5 | 231 | −0.0240 | 5 | 4.358 | YES |
| D | 4 | 285 | −0.0278 | 5 | 4.863 | NO |
| E | 9 | 498 | −0.0277 | 5 | 14.200 | NO |

5033-10/2-88[5-2]

The epoch vector at ignition for the long burn was propagated using the GTDS EPHEM Program to obtain a nominal ephemeris (solution N). A thrust calibration factor ($1 + \tau$) of 0.883 was used. Since the calibrated thrust was used, the magnitudes of the estimated $\tau$ in Table 6 are significantly smaller than the ones estimated during the calibration burn.

In addition to the thrust estimation, ephemeris comparisons were made analogous to those made for the calibration burn. In this case, the reference ephemeris reflects a calibrated thrust rather than the nominal thrust from the GMAN Program, so that the differences should be much smaller than those obtained for the calibration burn case. This is seen to be the case, with the position differences smaller than those observed in Table 5 by an order of magnitude or more. Detailed numerical results are available in Reference 4.

## 2.3 CONCLUSIONS

The conclusions from this thrust estimation study using the TTFM for the TEST and ERBS spacecraft are as follows:

- The TTFM is capable of modeling thrust application and estimation for the case of low thrust levels.
- The results for TEST establish that the thrust scale factor can be estimated to an accuracy of 1 percent.
- Measurement noise does not significantly influence thrust estimation.
- Target (TEST) or relay (TDRS) a priori state errors result in poor overall trajectory determination but adequate thrust level estimation.
- The results for TEST show that thrust estimation based on tracking measurements evenly distributed throughout the burn period or clustered away from the start of the burn period is more reliable than for other data distributions.

# 3. ATTITUDE-DEPENDENT THRUST ESTIMATION

This section describes the attitude-dependent thrust modeling for a spacecraft whose thrust direction maintains a fixed orientation with respect to the Sun. Specifically, the angle $\beta$ between the spin axis and the spacecraft-to-Sun line is fixed, while the spin axis is perpendicular to the position vector of the spacecraft. In the scenario used for this study, the total thrust is directed along the spin axis, so that there is a substantial out-of-plane component. The purpose of this study is to examine whether the thrust variation coefficient can be estimated in the presence of a large out-of-plane component, such as in this case. The formulation of this problem is discussed in Section 3.1, and the numerical results obtained using simulated tracking measurements are presented in Section 3.2.

## 3.1 METHOD FOR ATTITUDE-DEPENDENT THRUST ESTIMATION

For thrust estimation in the case of out-of-plane thrust, it is necessary to determine the components of the thrust acceleration in the orbital and inertial coordinate systems. This requires the determination of the time-varying yaw angle, $\alpha$, subject to the constraints mentioned previously. The resulting off-track and along-track thrusts are then estimated within GTDS, and a single calibration factor $(1 + \tau)$ is determined. The procedure for determining $\alpha$ is described in Reference 4.

Knowledge of $\alpha$ allows computation of the components of the total thrust, $A(t)$, in the orbital coordinate system. The along-track and cross-track components are $[A(t) \cos \alpha]$ and $[A(t) \sin \alpha]$, respectively. Transformation from the orbital coordinate system to the inertial coordinate system is straightforward and is described in Reference 1.

## 3.2 RESULTS AND DISCUSSION

The attitude-dependent thrust estimation capability was evaluated according to the plans used for along-track thrust estimation for the TEST spacecraft, with additional variation of the attitude. Simulated data were generated for the pass configuration shown in Figure 2. Range and Doppler tracking measurements were simulated for three cases, corresponding to values of $\beta$ equal to 95 degrees, 89 degrees, and 85 degrees. Tables 7 and 8 present summaries of the ephemeris comparison and differential correction results, using a Sun angle of 95 degrees, for mixed (range and Doppler) and Doppler-only tracking, respectively. Results using Sun angles of 89 degrees and 85 degrees show similar trends and are not presented here.

Table 7. Attitude-Dependent Long-Burn Thrust Solutions Using Range and Doppler Tracking

| PASS LENGTH (MINUTES) | COVARIANCE CONSTRAINTS | SOLUTIONS WITHOUT MEASUREMENT NOISE | | | SOLUTIONS WITH MEASUREMENT NOISE | | |
|---|---|---|---|---|---|---|---|
| | | ΔR AT TIME FROM EPOCH = $2^h\ 55^m$ | ΔR AT TIME FROM EPOCH = $6^h$ | FINAL THRUST SCALE FACTOR, $\tau$ | ΔR AT TIME FROM EPOCH = $2^h\ 55^m$ | ΔR AT TIME FROM EPOCH = $6^h$ | FINAL THRUST SCALE FACTOR, $\tau$ |
| 10 | YES | – | – | 0.11082097 | 0.685272 | 3.408705 | 0.10916828 |
| 20 | YES | – | – | 0.11104922 | - 0.512484 | - 2.406412 | 0.11241663 |
| 30 | YES | - 0.014102 | - 0.024721 | 0.11110209 | 0.075666 | 0.440116 | 0.11803708 |
| 40 | YES | - 0.008962 | 0.000991 | 0.11108741 | 0.014270 | 0.131255 | 0.11100793 |
| 50 | YES | - 0.007407 | 0.008889 | 0.11108283 | 0.000376 | 0.062123 | 0.11104714 |
| 60 | YES | - 0.007292 | 0.009374 | 0.11108285 | - 0.003369 | 0.043958 | 0.11105740 |
| 30 | NO | - 0.013935 | - 0.029438 | 0.11110237 | - 2.034615 | - 20.27488 | 0.13113265 |
| 40 | NO | - 0.014818 | - 0.032377 | 0.11110339 | - 6.832943 | - 48.90036 | 0.15156154 |
| 50 | NO | - 0.015987 | - 0.037745 | 0.11110653 | - 0.374978 | - 2.113980 | 0.11258244 |
| 60 | NO | - 0.017093 | - 0.041311 | 0.11110714 | - 0.013690 | 0.011517 | 0.11110525 |

5033-13/2-88 [5-2]

NOTES:

ΔR = ALONG-TRACK POSITION DIFFERENCES BETWEEN THE SOLUTION AND THE REFERENCE EPHEMERIS IN KILOMETERS.

THE "TIME FROM EPOCH" IS RELATIVE TO EPOCH $0^h$ ON 12/21/87.

Table 8. Attitude-Dependent Long-Burn Thrust Solutions Using Doppler Tracking

| PASS LENGTH (MINUTES) | COVARIANCE CONSTRAINTS | SOLUTIONS WITHOUT MEASUREMENT NOISE | | | SOLUTIONS WITH MEASUREMENT NOISE | | |
|---|---|---|---|---|---|---|---|
| | | ΔR AT TIME FROM EPOCH = $2^h\ 55^m$ | ΔR AT TIME FROM EPOCH = $6^h$ | FINAL THRUST SCALE FACTOR, $\tau$ | ΔR AT TIME FROM EPOCH = $2^h\ 55^m$ | ΔR AT TIME FROM EPOCH = $6^h$ | FINAL THRUST SCALE FACTOR, $\tau$ |
| 10 | YES | 0.089158 | 0.468314 | 0.11082982 | 0.700250 | 3.484579 | 0.10912462 |
| 20 | YES | 0.015790 | 0.117878 | 0.11102339 | - 0.522313 | - 2.449648 | 0.11244073 |
| 30 | YES | - 0.014962 | - 0.029045 | 0.11110457 | 0.119525 | 0.656288 | 0.11070862 |
| 40 | YES | - 0.008873 | 0.001277 | 0.11108731 | 0.014806 | 0.134985 | 0.11100535 |
| 50 | YES | - 0.007053 | 0.010416 | 0.11108205 | - 0.001797 | 0.043368 | 0.11106077 |
| 60 | YES | - 0.011071 | - 0.010362 | 0.11109407 | - 0.004126 | 0.031946 | 0.11106731 |
| 40 | NO | - 0.014547 | - 0.036515 | 0.11110770 | - 9.1509 | -74.52409 | 0.17437262 |
| 50 | NO | - 0.017205 | - 0.056732 | 0.11112461 | - 1.099791 | - 13.697040 | 0.12361447 |
| 60 | NO | - 0.017386 | - 0.060507 | 0.11112855 | - 0.019558 | - 0.68962 | 0.11187040 |

5033-14/2-88 [5-2]

NOTES:

ΔR = ALONG-TRACK POSITION DIFFERENCES BETWEEN THE SOLUTION AND THE REFERENCE EPHEMERIS IN KILOMETERS.

THE "TIME FROM EPOCH" IS RELATIVE TO EPOCH $0^h$ ON 12/21/87.

The tracking measurements used in evaluating the attitude-dependent thrust model (ADTM) were generated by the R&D GTDS Data Simulation (DATASIM) Program (with ADTM enhancements) for a total thrust profile determined by the GMAN Program. The estimations were performed using the GTDS DC Program, modified to include the ADTM enhancements. During the DC Program executions, the magnitude of the input thrust was scaled to 90 percent of the nominal (GMAN) thrust [$\phi = 0.9$, see Equation (10)], so that $\tau$ must have the value 0.111111 for good thrust estimation. The use of a single thrust scale factor, $\tau$, results in uniform scaling of all components of thrust.

Comparison of the ranges of $\tau$ for noise-free data in Tables 7 and 8 shows the two to be almost identical. The differences between the estimated $\tau$ and the ideal $\tau$ range from a maximum of 0.3 percent to a minimum of 0.004 percent for noise-free data. The better comparisons are associated with the longer data arcs. The thrust scale factors are also relatively insensitive to the presence or absence of constraints on the a priori state vector for the case of noise-free data.

This is significantly different from the corresponding results for data with measurement noise. With a constrained a priori state, the differences between $\tau$ and 0.111111 range from 2 percent to 0.04 percent, but the accuracy is greatly reduced by removing the constraint. For the latter condition, the difference ranges from a maximum of 57 percent, for the smallest data arc in the series (30 minutes), to a minimum of 0.1 percent, for the 60-minute data arc.

This trend is similar to the one observed for the case of along-track thrust; i.e., for the case of data with measurement noise, the final thrust estimation accuracy is very sensitive to the data arc length when the a priori state is also being estimated. These general trends are confirmed by the ephemeris comparisons, which are very large for the shorter data arcs with no covariance constraint and are smaller and relatively insensitive to the data arc length for the case of a constrained a priori state.

## 3.3 CONCLUSIONS

The following conclusions can be made from the study of attitude-dependent thrust estimation presented above:

- In the case of attitude-dependent thrust, the use of a covariance matrix to fix the initial state vector ensures a reliable estimation of the thrust scale factor using a 10-minute TDRS-W tracking pass beginning 15 minutes from ignition.

- If the state vector and $\tau$ are both estimated (i.e., no a priori state covariance constraint is imposed), noise has a considerable effect on the reliability of the solution. If the initial state vector is constrained, however, noise has very little effect.

- To obtain reliable estimates of the state vector and $\tau$, an observation timespan of at least 50 minutes is generally needed.

# 4. FUTURE DEVELOPMENTS IN THRUST ESTIMATION

Many future missions will make greater demands on the thrust estimation capability of trajectory determination systems. The increased sophistication of spacecraft tracking systems, stricter accuracy requirements, and more complicated attitude and thrust schedules will require thrust estimation systems to provide calibration factors on a near-realtime basis and for more general attitude acquisition scenarios. It would be desirable to have a system capable of handling attitude information from a variety of sources.

The conclusions stated here apply strictly to only the low-thrust, long-burn case. For the case of high-thrust perturbations, numerical problems, associated with the start and end of the burn period, can be anticipated. Analysis is currently being performed to determine if the status of low-burn thrust estimation in GTDS applies to the high-thrust case.

## ACKNOWLEDGMENTS

The authors wish to acknowledge the assistance of the following Computer Sciences Corporation personnel: T. Lee, L. J. Bellantoni, H. L. Hooper, and E. J. Smith.

## REFERENCES

1. Goddard Space Flight Center, X-582-76-77, Mathematical Theory of the Goddard Trajectory Determination System, J. O. Cappellari, Jr., C. E. Velez, and A. J. Fuchs (editors), April 1976

2. Computer Sciences Corporation, CSC/SD-85/6738, Goddard Trajectory Determination System (GTDS) User's Guide, Revision 2, D. Squier and K. Byers, December 1985

3. Computer Sciences Corporation, CSC/TM-85/6741, Study of Orbit Estimation Techniques, P. S. Lee, S. M. Kirschner, and A. S. Lyubomirsky, December 1987

4. Computer Sciences Corporation, CSC/SD-86/6724, Selected Topics in Orbit Determination, S. M. Kirschner, L. J. Bellantoni, and A. S. Lyubomirsky, January 1987